POLARIS SEMICONDUCTOR

Application Note
PSAN001

Switching-Free Boost Regulators: A Compact, All-Linear Solution to Stepping-Up Voltage

K. Schmieder
M. Lumb

SEPTEMBER 2025

At a Glance

Introduction

DC boost voltage regulators have vast applications across a wide variety of electronics markets. They serve a critical function in providing a precisely regulated voltage that exceeds that of the input. The importance of this is particularly salient in battery-powered portable systems, where one is often limited by an energy source below 4 V (e.g. single-cell Li-Ion) that needs to power 5V loads. Some examples across industries include medical wearables for heart rate and/or pulse oximetry [1, 2], environmental CO_2 sensors [3, 4], electronics for automotive systems under cold crank conditions [5], display power management [6], Bluetooth and LoraWAN sensors/transmitters [7], and low-power energy harvesters [8].

Incumbent technologies for DC voltage boosting broadly fall into one of three categories: inductor-based boost converters, switched-capacitors, or transformer-based. Each of these established technologies offers a distinct set of advantages and disadvantages, often forcing engineers into a series of design trade-offs.

Inductor-based boost converters are valued for their high efficiency and power delivery capabilities, making them a common choice in many applications. However, this performance is accompanied by significant electromagnetic interference (EMI) generated by the rapid switching inherent to their design. In sensitive analog systems, RF circuits, and precision equipment, this switching noise degrades performance and necessitates bulky, expensive filtering and shielding to maintain system integrity. Furthermore, the magnetic components central to their operation contribute to a larger solution footprint.

On the other hand, switched-capacitor converters offer a more compact and often lower-cost alternative, free from the magnetic elements that plague their inductor-based counterparts. Their inherent design generates less EMI, making them an attractive option for moderately noise-sensitive applications. The trade-off, however, often lies in their limited output current capabilities and a potential decrease in efficiency, particularly as the output voltage requirement deviates from simple integer multiples of the input voltage. Ultimately, for the most demanding low-noise applications, both inductor-based and switched-capacitor converters often require a final-stage linear regulator, which in-

IN BRIEF

Engineers have long faced a tradeoff in DC boost conversion, balancing the competing demands of efficiency and power delivery against solution footprint and noise. Polaris Semiconductor's Enhanced Linear Regulator offers a new architecture to resolve these compromises.

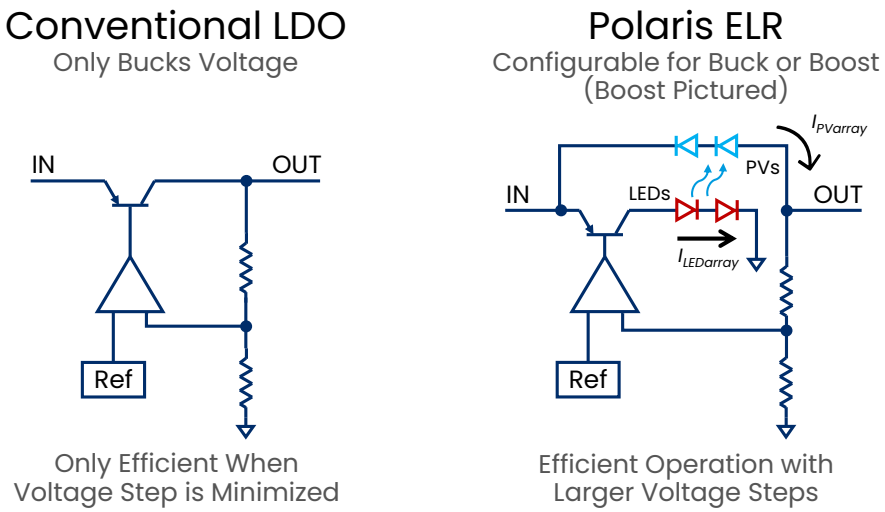

Figure 1. *Circuit topology for a conventional LDO (left panel) and a Polaris Semiconductor ELR operating in boost-mode (right panel).*

creases solution size and cost while reducing overall system efficiency.

For applications requiring safety isolation or very high voltage step-up ratios, designers often turn to transformer-based topologies like flyback or forward converters. While these provide excellent galvanic isolation, they are inherently complex and still rely on high-frequency switching, thereby sharing the same fundamental drawbacks of EMI generation that can interfere with sensitive electronics. In systems that require low-noise performance, such as RF, precision sensing, audio, medical devices, and many more, incumbent approaches leave a clear gap for a solution that can provide a voltage boost without the penalty of switching noise.

Polaris Semiconductor's Enhanced Linear Regulator (ELR) addresses these problems directly. This inductorless and entirely switching-free technology enables efficient step-down and step-up conversion while retaining the low-noise and small footprint/bill of materials (BoM) benefits of conventional low-dropout (LDO) voltage regulators. This application note serves to introduce a straightforward and versatile configuration of the technology for stepping-up voltage—in addition to detailed analyses of ripple rejection and output noise—offering a new tool to designers seeking boost conversion without the traditional compromises in noise and complexity.

Boost ELR Overview

For a deep-dive of the underlying technology, we encourage the reader to check out our accompanying white paper, **Breaking the Rules of Linear Regulators** [9]. Herein, we provide a high-level overview before advancing to an interesting boost ELR design and its associated performance.

Fundamental Principles

Our patented device architecture comprises a conventional, Si-based LDO, co-packaged with Polaris Semiconductor's unique, high-performance, GaAs-based photovoltaic-output optocouplers in a multi-chip module. The role of the optocoupler is to transfer optical power from the LED section to the photovoltaic (PV) device with high efficiency.

In a conventional LDO, a pass transistor is used to create a controlled voltage drop between the input and output terminals. Due to the resistive nature of using the pass transistor to regulate the output, the output voltage must always be lower than the input (**Figure 1**). In

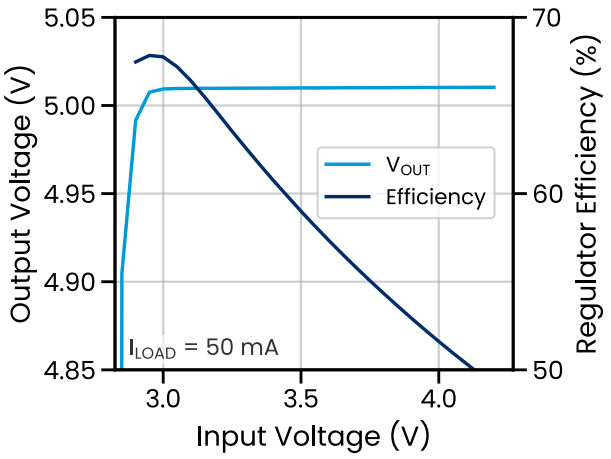

Figure 2. *Output voltage (primary y-axis) and regulator efficiency (secondary y-axis) plotted as a function of input voltage for BT291D50M.*

Polaris Semiconductor's ELR, the pass transistor supplies current to the LED sections of arrayed optocouplers, which is efficiently transferred to photocurrent in the the PV array via photons emitted in the LEDs. The PV devices are connected to the input and output terminals of the regulator, enabling the output voltage to exceed the input voltage. As with conventional LDOs, the ELR output voltage is tightly regulated thanks to a feedback circuit that senses the output voltage and—leveraging an error amplifier and reference—adjusts the pass transistor accordingly.

Boost Tech Performance Comparison

For typical applications involving a single-cell Li-ion battery requiring 5V boost, the ELR topology facilitates efficiencies in the range of 55%–65% (**Figure 2**). For a similar load current, a voltage doubler switched-capacitor solution might be up to 5% absolute higher efficiency than the ELR. However, this improvement comes at the cost of introducing switching EMI, poorer transient response, and limited output current. If the device is powering a load with stringent noise/transient specifications, a linear post-regulator might be required—lowering system efficiency. Inductor-based boost converters achieve the highest efficiencies of greater than 90%; however, their conducted and radiated EMI is a challenge to mitigate, and the inductor—in addition to other passives—increases footprint, BoM, as well as overall complexity. Inductor-based converters can also be followed by linear post-regulators to mitigate the effects of conducted EMI, but this has downsides in the reduction to efficiency and further footprint/BoM increase. These three power architectures for achieving a regulated, low-noise 5V output from a single-cell Li-based battery are depicted in **Figure 3**.

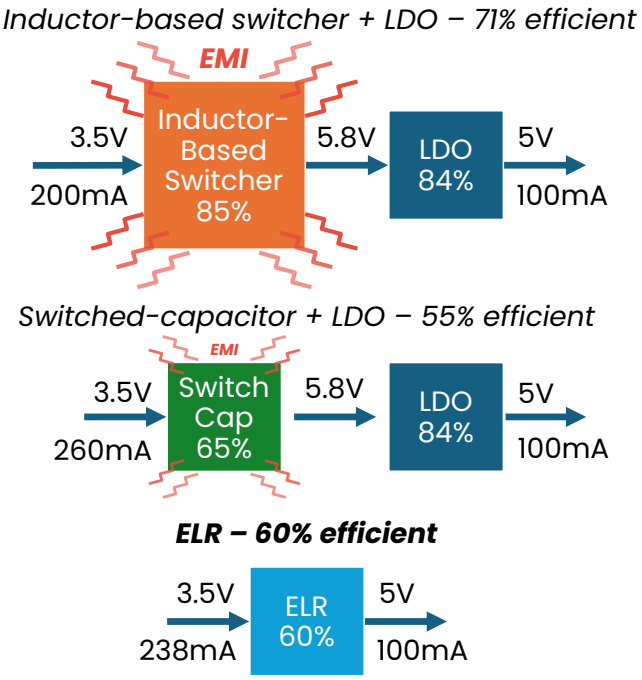

Figure 3. *Performance comparison of incumbent technologies versus the Polaris Semiconductor approach to low-noise boost regulators.*

Building With Boost ELRs

The preceding overview established how the ELR architecture provides efficient, low-BoM, switching-free boost conversion. To demonstrate how this theory translates into a practical solution, the remainder of this note will focus on a design example using a specific component: the Polaris Semiconductor **BT291D50M**.

This versatile ELR is built around a general-purpose bipolar LDO, enabling an adjustable, regulated output of up to 5V, a maximum load current of 350 mA, and a min-

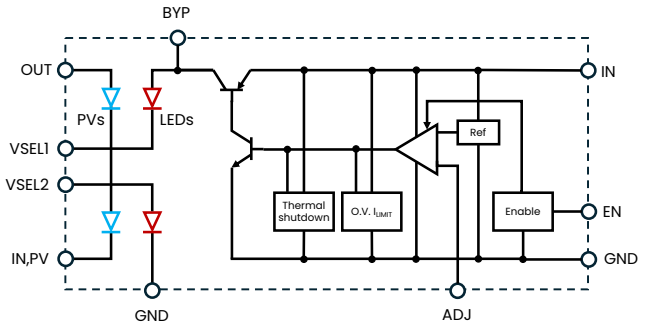

Figure 4. *Functional block diagram for BT291D50M.*

imum input voltage of approximately 3V (minimum input voltage varies with load current and temperature—see **Figure 9**). Housed in a 6 mm × 6 mm QFN-28 package, it features low ground current, good low-frequency PSRR, and useful protection functions like over-current and over-voltage protection. Its combination of performance and small footprint makes the chip ideal for switching noise-sensitive and space-constrained applications, from industrial IoT and medical wearables to portable electronics. The device is also radiation tolerant, suiting it for applications in low-Earth orbit (LEO).

The following sections will provide a detailed walk-through of the BT291D50M's functional description, external component selection, PCB layout, and measured performance.

Functional Description

The functional block and pinout diagrams, respectively, of BT291D50M are provided in **Figures 4–5**. Most elements in these diagrams will be highly familiar to those experienced with LDOs. The IN pins (20, 21) are tied to the emitter of the PNP pass transistor and carry a portion of the input current. IN,PV pins (10, 11) carry the remainder of the input current, and are tied to the negative terminal of the PV array. The EN pin (19) can set an input supply undervoltage lockout (UVLO) threshold using a resistor divider; however, it can simply be tied to the IN pins if this functionality is not desired. The ADJ pin (13) provides feedback for setting the output voltage. This is typically connected to a resistor divider that is tied to the output. The GND pins (5, 6, 16, 17, and thermal

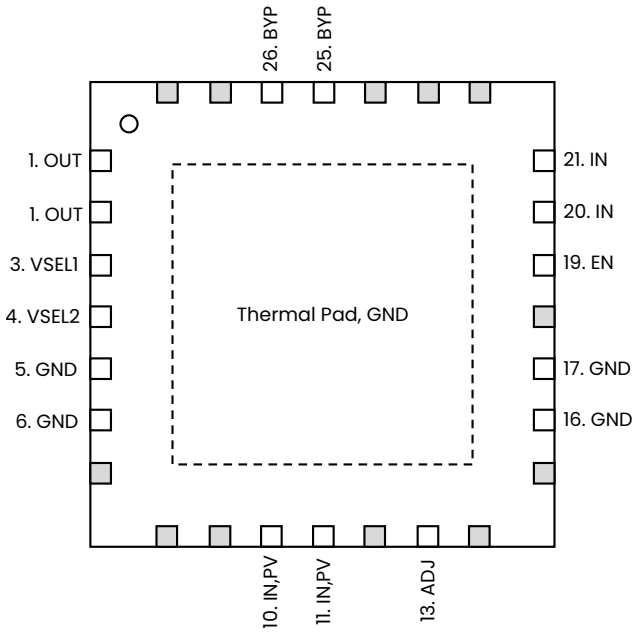

Figure 5. *Pinout diagram for BT291D50M.*

pad) should all be tied to the PCB's ground plane. The OUT pins (1, 2) are internally connected to the positive terminal of the PV array and supply the load's regulated output. The BYP (25, 26) pins share a node with the pass transistor's collector and the positive terminal of the first LED. The BYP pins can be used to operate the device as a conventional LDO. However, they are not used in this application note and should be tied together and not be tied to anything else. The VSEL1 (3) and VSEL2 (4) pins must be tied together to series-connect the LED array and facilitate boost functionality; these pins should not be tied to anything else.

Typical Application

A schematic for BT291D50M is provided in **Figure A1**, intended for boosting a common single-cell Li-based battery to a regulated 5V. This schematic is the basis for the demonstration board discussed in the following sections. While not required for sources such as Li-based batteries, a 0.1 µF input bypass capacitor between IN and GND is recommended for input sources with high AC impedance. At the output of the device, a minimum 22 µF output capacitor is required to stabilize the control loop. X7R or X5R type capacitors are

recommended due to their wide temperature spec and low temperature coefficient. For ceramic capacitors with very low equivalent series resistance (ESR), it is recommended to include a low value resistor (e.g. 0.47 Ω) in series with the capacitor to improve loop stability (not pictured). We selected tantalum output capacitors in this application note to provide effective loop stability and sufficient ESR. Finally, the 5V output voltage is set via two resistors that serve as a resistor divider at the ADJ pin. The output voltage for given resistor values can be calculated as follows:

$$V_{OUT} = 1.240 \left(\frac{R_1}{R_2} + 1 \right) \quad (1)$$

Where R1 connects between OUT and ADJ, and R2 connects between ADJ and GND. This equation can be re-arranged as follows:

$$R_1 = R_2 \left(\frac{V_{OUT}}{1.240} - 1 \right) \quad (2)$$

The ADJ pin has high input impedance and therefore large resistor values can be used up to 1 MΩ. While higher resistor values reduce current consumption under light load conditions, there is a minimum load current requirement for the LDO to avoid a rise in output voltage under very light load. The combination of R1=14.7 kΩ and R2=4.87 kΩ effectively balances these priorities.

A Tiny Boost Regulator

To illustrate the size, weight, and power (SWaP) benefits of the regulator, we built BT291D50M (hereafter referred to as BT29[1]) evaluation boards with a total solution size of 12.5 mm × 7.5 mm (**Figure 6**) (the full board is 13.6 mm × 13.3 mm). The tallest component, the output capacitor, measures only 1.2 mm in height—all other components including the ELR are sub-1 mm in height. This board uses only four passive components: an input capacitor (optional), an output capacitor, and a resistor divider to set the output voltage. And yet, despite its simplicity and minimal footprint, this chip represents an efficient method to deliver 5V (**Figure 2**)—with none of the switching EMI challenges.

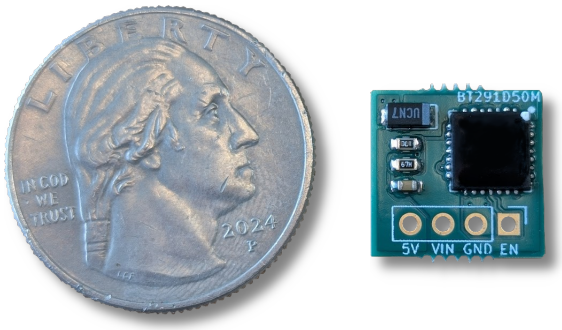

Figure 6. *Polaris Semiconductor's BT29 5V linear boost regulator with a 12.5 mm × 7.5 mm × 1.2 mm solution size, including a total of four passives.*

PCB Layout

The PCB layout is provided in **Figure 7**. The board was designed to maximize simplicity and minimize footprint. The 0.1 in-pitch plated through holes are compatible with standard header pins and provide access to IN, OUT, GND, and EN. The board features two copper layers, with the back copper layer being used almost entirely as a ground plane to help spread heat. The board has a minimum drill hole size of 0.3 mm diameter. While we generally recommend that the thermal vias under our QFN part have a smaller hole size (we use 0.255 mm diameter thermal vias on our other evaluation boards), we opted for 0.3 mm on this breakout board to minimize cost across the widest range of PCB manufacturers. Smaller thermal vias reduce risk of solder volume loss. These losses can be eliminated by plugging vias, or partially mitigated by tenting. To learn more about thermal pad via design, we can recommend a number of excellent resources [10, 11, 12].

[1]Our part numbers begin with two letters indicating the product category (BT for boost regulator), followed by two numbers for the product family (29). Thus, BT291D50M is the full part number from our BT29 product family that is optimized for 5V output from a single-cell Li-ion input.

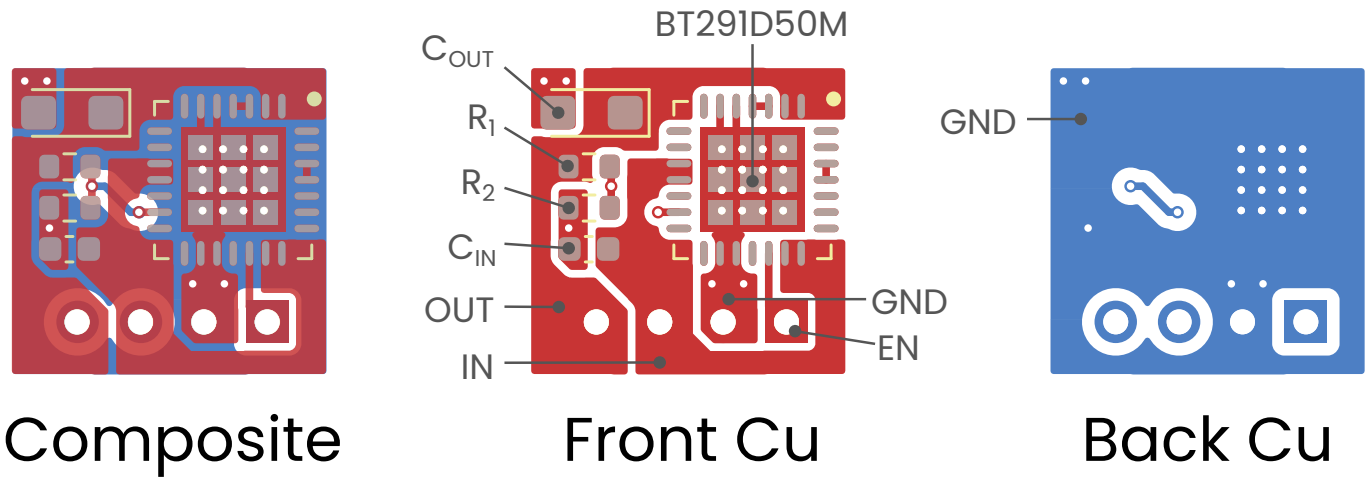

Figure 7. *PCB layout for "Tiny Boost" Board. Red fills represent front copper, blue fills represent back copper, and gray fills represent the front solder paste.*

All PCB design files from this Application Note are available for download on our website. The full BoM for this board is provided in **Table 1**. We selected a tantalum output capacitor to ensure effective loop stability and sufficient ESR. The input capacitor is X7R ceramic.

Performance

Electrical measurements were made using a pulsed input bias with a 10 ms on-time and 50 ms off-time to reduce heating during test. The efficiency as a function of load current is depicted in **Figure 8**. For a given input voltage, the efficiency is highly stable across a range of typical load currents. For battery sources with inputs voltages below 3.7 V and 3.4 V, respectively, efficiencies are in excess of 55% and 60%. Additionally, the performance can be further improved by optimizing the board thermal characteristics. We opted for the most easily manufacturable and smallest practical form factor; however, increasing the number of copper layers, the copper weight per layer, or the overall PCB size will yield further performance improvements via enhanced heat spreading.

Important considerations for the applications engineer are the maximum anticipated load current and board temperature. Note that the input voltage range is dependent upon the load current. This occurs because

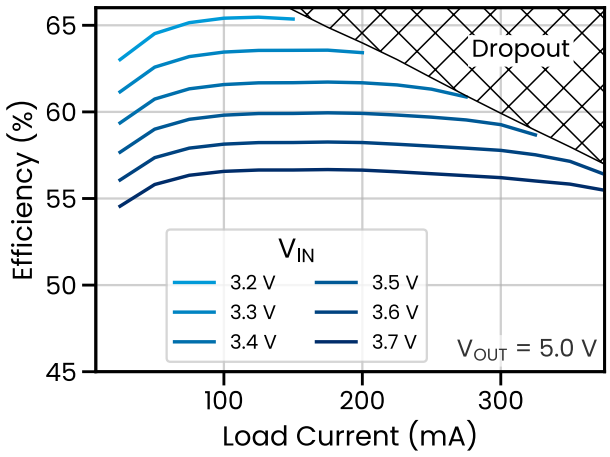

Figure 8. *BT29 "Tiny Boost" efficiency versus load current for various input voltages, 25°C operation. Not all input voltages are compatible with the full load current range, as indicated by the hatched dropout region.*

the turn-on voltage is the sum of the dropout voltage of the LDO (V_{DO}) in addition to the forward voltage drop across the LED array, which are both current dependent (see the right panel of **Figure 1**). Lower input voltages have a more limited range of load currents in which a regulated output can be produced before the device enters dropout.

$$V_{ON} = V_{DO} + V_f\left(I_{LED,Array}\right) \quad (3)$$

Table 1. *Bill of Materials for the Tiny Boost board.*

ID	Description	Part	Manufacturer
C_{IN}	0.1 μF ceramic X7R	CL10B104KB8NNWC	Samsung
C_{OUT}	33 μF tantalum poly.	T527S336M016ATE200	Kemet
R_1	14.7 kΩ 0.5% 1/16W	RR0816P-1472-D-17C	Susumu
R_2	4.87 kΩ 0.5% 1/16W	RR0816P-4871-D-67H	Susumu
U_1	5V Linear Boost Regulator	BT291D50M	Polaris Semiconductor

The turn-on voltage is defined as the minimum input voltage to produce a regulated output voltage. Since LED forward voltage increases with injection current, the variation in turn-on voltage is greater than the LDO dropout alone. BT29's turn-on behavior for a regulated 5V output is plotted in **Figure 9**. At the maximum rated output voltage of 5 V and maximum junction temperature of 125°C, the turn-on voltage increases significantly due to the optocouplers having reduced efficiency and lower maximum power voltage. For Li-ion powered applications where ELR device temperatures close to the 125°C maximum are anticipated, we suggest limiting the maximum output current to 200 mA or below to keep V_{ON} low. A lower output voltage of 4.5 V or below also significantly lowers efficiency losses due to the optocouplers at high temperature, reducing dissipated power and lowering V_{ON}. The thermal protection feature of the internal LDO protects the device in case maximum temperature is exceeded, preventing thermal runaway. A method for calculating thermal design metrics for ELR devices will be the subject of a future application note.

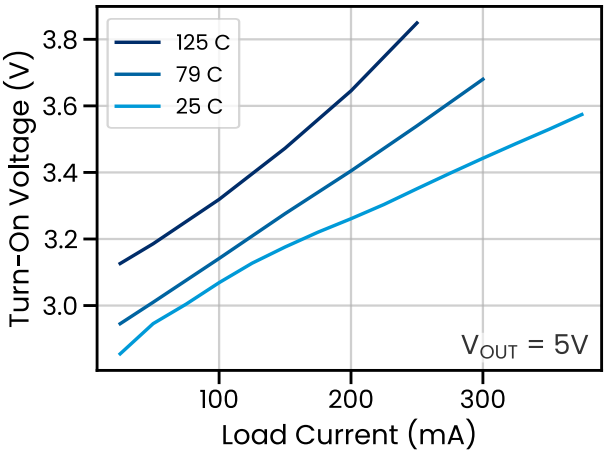

Figure 9. *Minimum input voltage required to produce a regulated 5V output, plotted as a function of load current at various device temperatures.*

Linear Boost PSRR & Noise

In the boost ELR topology, the conventional LDO feedback loop is substantially reconfigured. The connection of the pass transistor to the output terminal is broken, and the feedback loop is completed by the photocurrent flowing between the LEDs and the PVs then to the output. This has interesting implications for PSRR and noise performance, which are in-part dictated by the feedback circuit and loop gain. To examine the effect of this altered configuration, we have compared the PSRR and spectral noise density of our BT29 "Tiny Boost" ELR versus that of the same LDO part operating in conventional buck mode. As a reminder, to build an ELR we co-package a conventional LDO with our highly efficient optocouplers in a unique circuit layout. Thus, we can isolate the effect of optocouplers and the reconfigured feedback loop by evaluating noise performance of the boost ELR versus the underlying buck LDO. For these measurements, we chose to use the same passives for the conventional LDO as we used for the boost ELR (see Table 1). Both the ELR and conventional LDO were designed to output 5 V for this experiment. Note that the evaluation board designs

were quite different between the two chips. However, the same design principles of placing passives close to the device pins and using low impedance copper pours for input, output and ground planes were followed.

PSRR at a variety of load currents is shown in the top panel of **Figure 10** for both BT29 (solid lines) and the underlying LDO operating in buck mode (dashed lines). It is evident that boost mode ELR's do incur some PSRR penalty; however, it is small. In the low frequency regime in which PSRR is typically dictated by a combination of bandgap and loop gain, the PSRR difference amounts to approximately 5 dB. Thus, the BT29 Tiny Boost ELR board is still managing 65 dB of ripple rejection despite a circuit topology with the pass transistor not directly connected to the output pin. The PSRR roll-off behavior is slightly shifted to lower frequency in the ELR, while the slope remains relatively unchanged. At higher frequencies, performance of the two regulators diverges. While the standalone LDO's PSRR improves as its output capacitor shunts ripple to ground, this effect in BT29 appears somewhat muted.

In the bottom panel of **Figure 10**, the same BT29 PSRR is plotted as a function of input voltage at 50 mA load current. The PSRR is mostly stable for input voltages of 3.1 V and above. Note that this also includes input voltages exceeding the 5 V output voltage. The boost-mode ELR in fact does act as a buck regulator at these higher voltages; however, it does so at lower efficiency[2]. At input voltages below approximately 3.1 V, the PSRR drops in a similar fashion to conventional LDOs operating near dropout. Upon inspection of **Figure 9**, the turn-on voltage at 50 mA is approximately 2.9 V, suggesting that an additional 200 mV is necessary to achieve a regulated output with high PSRR.

We can now turn our attention to the noise spectral density plots in **Figure 11**. Once again, we are comparing

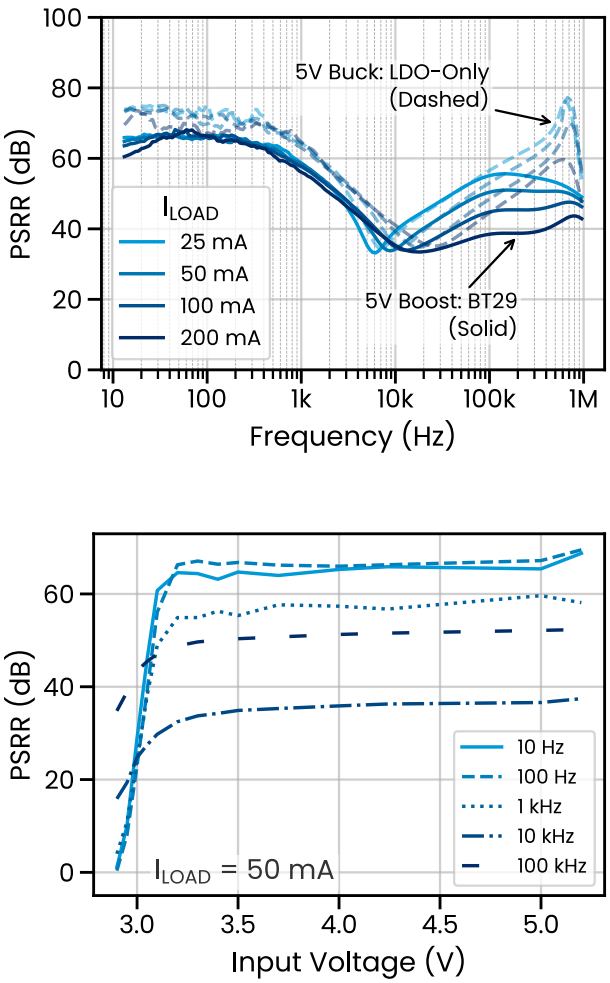

Figure 10. *BT29 "Tiny Boost" power supply ripple rejection versus frequency (top panel) and input voltage (bottom panel).*

BT29 to the underlying conventional LDO in buck mode, where both chips are operating at 100 mA load current. At frequencies below approximately 4 kHz, the output noise of the boost-mode ELR matches that of the conventional LDO. In this low-frequency regime, the voltage reference and error amplifier are typically the dominant noise sources, suggesting that their contribution to noise has not been significantly altered by the optocouplers and boost ELR topology. The roll-off in bandwidth-limited noise begins slightly earlier in the case of BT29. Of note is the peaking in output noise that occurs only for the conventional LDO. This is typically associated with suboptimal compensation. Recall that

[2]You might be wondering whether the concept of a boost ELR can be combined with a conventional LDO that bypasses the optocouplers when V_{IN} is above the dropout voltage, producing a highly efficient buck regulator when V_{IN} is slightly greater than VOUT. The answer is yes—stay tuned for a future application note on buck-boost ELRs!

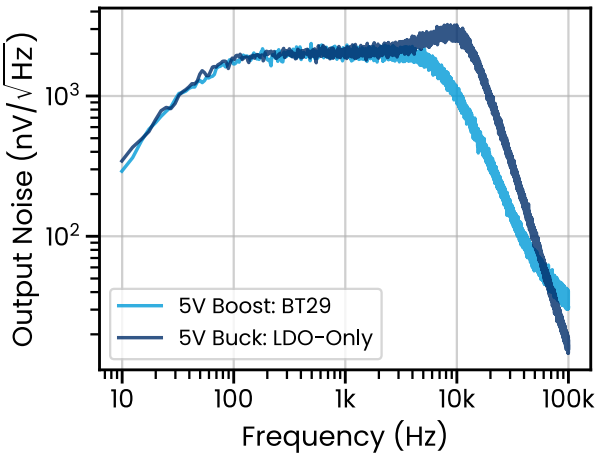

Figure 11. *Spectral noise density of BT29 in boost mode compared with its underlying LDO operating in buck mode. Load current and output voltage are 100 mA and 5V, respectively.*

we chose to use the same passive components for both the LDO and the ELR to isolate the effect of optocouplers and altered topology. One drawback of this approach was suboptimal stability for the standalone LDO. While the LDO requires an output capacitor with some ESR for stability, the one we chose may have been insufficient for the conventional buck LDO, while still being acceptable for the boost ELR[3]. By replacing the buck LDO board's tantalum output capacitor with a ceramic capacitor followed by a small series resistor (e.g. 0.47 Ω), we can improve the phase margin and eliminate this minor instability (not pictured). Nevertheless, it is instructive to see that—given the difference in unity gain—the boost ELR was slightly easier to stabilize than the standalone LDO.

The total integrated noise (10 Hz – 100 kHz) of BT29 and the standalone LDO, respectively, registered 213 µV RMS and 327 µV RMS for an identical BoM including a 33 µF tantalum output capacitor. Ignoring the resonant peaking that occurs in the standalone LDO, these data suggest that ELRs operating in boost mode will have noise performance that largely matches that of the underlying LDO. Further supporting this, we re-purposed the Tiny Boost board for assembly of a BT19 boost ELR outputting 5V (Polaris Semiconductor's **BT191D50M**). The total integrated noise of BT19 registered 78 µV RMS, matching the specification sheet noise performance of its underlying LDO. A summary of noise performance is provided in **Table 2**. We also included an additional measurement of BT29 using a larger output capacitor, illustrating that—much like conventional LDOs—the noise performance can be improved with appropriate selection of passive components.

Table 2. *RMS output noise summary for various LDO and ELR designs at 5V output and 100 mA load current.*

Product Family	Output Cap	Configuration	Output Noise[4]
BT29	33 µF tantalum	Buck: LDO-Only	327 μV_{RMS}
		Boost: ELR	213 μV_{RMS}
	47 µF tantalum	Boost: ELR	173 μV_{RMS}
BT19	33 µF ceramic[5]	Boost: ELR	78 μV_{RMS}

Overall, these PSRR and spectral noise density comparisons suggest that—for the first time—engineers can achieve boost-mode regulation from a single chip with nearly identical noise and ripple rejection to LDOs in step-down mode. The major factor controlling the noise and ripple rejection of these ELRs is the underlying LDO. Given that our optocouplers can be integrated into nearly any LDO architecture, the design space is wide-open for building step-up voltage regulators with performance metrics to suit your application[6].

Conclusion

This application note has introduced Polaris Semiconductor's Enhanced Linear Regulator (ELR) as a prac-

[3]The datasheet for T527S336M016ATE200 indicates an ESR of approximately 0.2 Ω at 10 kHz

[4]Integrated RMS output noise within the range of 10 Hz – 100 kHz

[5]BT19's LDO does not have the same minimum-ESR output capacitor requirements that BT29's has. Thus, a ceramic output capacitor was most appropriate.

[6]Are you looking for even lower output noise than that provided by BT19 or BT29? Reach out at info@polarissemiconductor.com and let us know your boost ELR requirements.

tical and compact solution for stepping up voltage without the drawbacks of traditional switching converters. By leveraging a unique co-packaged architecture of conventional LDOs with high-efficiency optocouplers, the ELR enables boost regulation that is inherently switching-free, minimizing EMI while maintaining a small footprint and simple bill of materials.

Through the BT291D50M "Tiny Boost" example, we demonstrated how this technology delivers regulated 5 V outputs from single-cell Li-based sources with a total solution size of $12.5 \times 7.5 \times 1.2$ mm^3 and efficiencies in the 55–65% range—sufficient for many space-constrained and noise-sensitive applications where inductor-based or switched-capacitor converters pose challenges. Importantly, the ELR achieves noise and PSRR performance nearly indistinguishable from its underlying LDO, giving engineers confidence in precision and sensitive analog system designs.

The combination of simplicity, compact size, radiation tolerance, and low noise makes boost ELRs particularly well-suited for wearables, IoT devices, medical instrumentation, and aerospace applications. As Polaris Semiconductor continues to expand its ELR product family, designers now have a versatile, linear alternative to conventional boost topologies—providing new degrees of freedom in balancing efficiency, noise, and solution footprint.

Appendix

BT291D50M Schematic

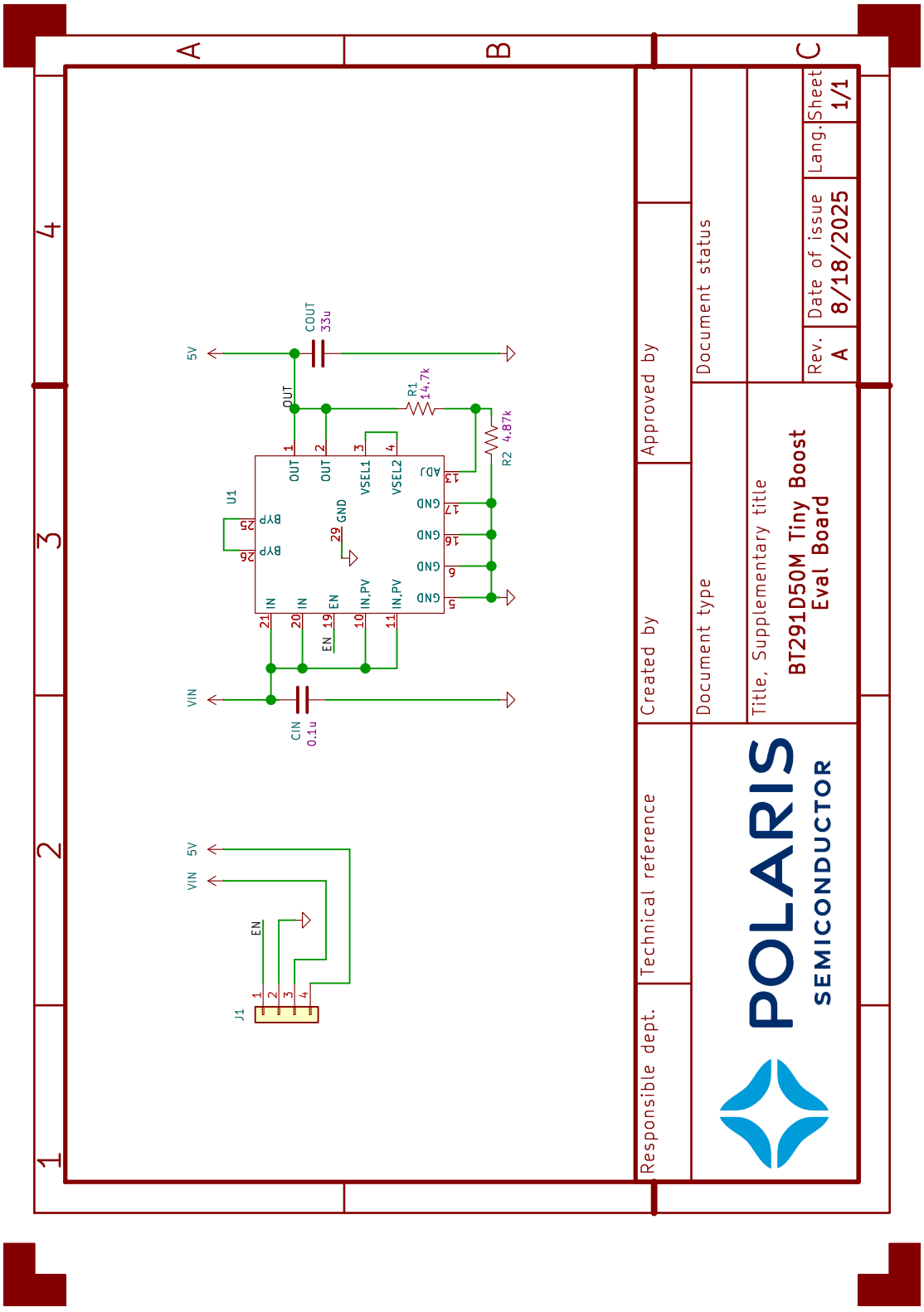

Figure A1. *Schematic for tiny boost board.*

References

[1] M. Jackson and F. Dowling, "Choose the proper PMIC to boost your optical sensor SNR," Application Note 7035, Maxim Integrated, 2019.

[2] *AFE4400 and AFE4490 Development Guide*, User's Guide SLAU480C, Texas Instruments, 2014.

[3] "Design-in guidelines for XENSIV™ PAS CO2 gas sensors," Application Note AN213134, Infineon Technologies AG, 2025.

[4] S. P. Koyyala. (2025) ESP32 MH-Z19B: Building a DIY CO_2 monitor for smarter air quality projects. Circuit of Things. [Online]. Available: https://circuitofthings.com/esp32-mh-z19b-building-a-diy-co%E2%82%82-monitor-for-smarter-air-quality-projects/

[5] G. Roecker, "Maintaining output voltage regulation during automotive cold-crank with LM5118 buck-boost," Application Report SNVA741, Texas Instruments, 2015.

[6] "How to power the automotive TFT-LCD displays of the (not so distant) future," Design Solutions No. 122, Maxim Integrated, 2018.

[7] "Choose the right buck-boost for your IOT tracker," Application Note 7002, Maxim Integrated, 2014.

[8] D. Newell and M. Duffy, "Review of power conversion and energy management for low-power, low-voltage energy harvesting powered wireless sensors," *IEEE Transactions on Power Electronics*, vol. 34, no. 10, pp. 9794–9805, 2019.

[9] M. P. Lumb, K. J. Schmieder, J. DeLombard, J. Carlin, L. Kaliszewski, A. Price, D. Hollingshead, and T. Grassman, "Breaking the rules of linear regulators: High efficiency buck and boost conversion without switching," White Paper PSWP001, Polaris Semiconductor, 2025.

[10] S. Kummerl, B. Lange, and D. Nguyen, "QFN and SON PCB attachment," Application Note SLUA271C, Texas Instruments, 2023.

[11] Y. B. Quek, "QFN layout guidelines," Application Note SLOA122, Texas Instruments, 2006.

[12] D. Herron, Y. Liu, and N.-C. Lee. (2011) Pad design and process for voiding control at QFN assembly. IPC APEX EXPO. [Online]. Available: https://www.electronics.org/system/files/technical_resource/E6%26S03_02.pdf

Contact Us

Website: www.polarissemiconductor.com

Email: info@polarissemiconductor.com

Phone: +1 (571) 527-5928

Address: 1800 Diagonal Rd. Ste 600
Alexandria, VA 22314